European Journal of Pharmaceutics and Biopharmaceutics 136 (2019) 29–37

Contents lists available at ScienceDirect

European Journal of Pharmaceutics and Biopharmaceutics

journal homepage: www.elsevier.com/locate/ejpb

Research paper

Tumor recognition of peanut agglutinin-immobilized fluorescent nanospheres in biopsied human tissues

Hironori Kumagai[a,b], Kosuke Yamada[a], Kanako Nakai[a], Tokio Kitamura[a], Kohta Mohri[a,1], Masami Ukawa[a], Takumi Tomono[a], Takaaki Eguchi[c], Testuya Yoshizaki[c], Takumi Fukuchi[c,2], Takuya Yoshino[d], Minoru Matsuura[e], Etsuo Tobita[b], Wellington Pham[f,*], Hiroshi Nakase[g,**], Shinji Sakuma[a,***]

[a] Faculty of Pharmaceutical Sciences, Setsunan University, Hirakata 573-0101, Japan
[b] Life Science Materials Laboratory, ADEKA Corp., Tokyo 116-8554, Japan
[c] Department of Gastroenterology and Hepatology, Osakafu Saiseikai Nakatsu Hospital, Osaka 530-0012, Japan
[d] Division of Inflammatory Bowel Disease, Digestive Disease Center, Tadzuki Kouhuukai Kitano Hospital, Osaka 534-8680, Japan
[e] Division of Endoscopy, Kyoto University Hospital, Kyoto 606-8507, Japan
[f] Department of Radiology, Vanderbilt University Institute of Imaging Science, Nashville, TN 37232-2310, USA
[g] Department of Gastroenterology and Hepatology, Sapporo Medical University School of Medicine, Sapporo 060-0061, Japan

ARTICLE INFO

Keywords:
Diagnostic agent
Nanosphere
Peanut agglutinin
Colorectal cancer
Thomsen-Friedenreich antigen
Optical imaging
Biomarker imaging

ABSTRACT

We are investigating an imaging agent for early detection of colorectal cancer. The agent, named the nanobeacon, is coumarin 6-encapsulated polystyrene nanospheres whose surfaces are covered with poly(N-vinylacetamide) and peanut agglutinin that reduces non-specific interactions with the normal mucosa and exhibits high affinity for terminal sugars of the Thomsen-Friedenreich antigen, which is expressed cancer-specifically on the mucosa, respectively. We expect that cancer can be diagnosed by detecting illumination of intracolonically administered nanobeacon on the mucosal surface. In the present study, biopsied human tissues were used to evaluate the potential use of the nanobeacon in the clinic. Prior to the clinical study, diagnostic capabilities of the nanobeacon for detection of colorectal cancer were validated using 20 production batches whose characteristics were fine-tuned chemically for the purpose. Ex vivo imaging studies on 66 normal and 69 cancer tissues removed from the colons of normal and orthotopic mouse models of human colorectal cancer, respectively, demonstrated that the nanobeacon detected colorectal cancer with excellent capabilities whose rates of true and false positives were 91% and 5%, respectively. In the clinical study, normal and tumor tissues on the large intestinal mucosa were biopsied endoscopically from 11 patients with colorectal tumors. Histological evaluation revealed that 9 patients suffered from cancer and the rest had adenoma. Mean fluorescence intensities of tumor tissues treated with the nanobeacon were significantly higher than those of the corresponding normal tissues. Correlation of magnitude relation of the intensity in individuals was observed in cancer patients with a high probability (89%); however, the probability reduced to 50% in adenoma patients. There was a reasonable likelihood for diagnosis of colorectal cancer by the nanobeacon applied to the mucosa of the large intestine.

1. Introduction

Colorectal cancer is the third leading cause of cancer in the U.S.A. [1]. It is the second leading cause of death by cancer in Japan since the country adapts significantly more western diet [2,3,4]. Colonoscopy has been recognized as a golden tool for the detection of colorectal cancer [5]. The technique relies on the visualization of morphological changes such as polyps and adenocarcinoma in colonic tissues, while being leveraged by other assistive functions incorporated in the system, such as optical magnification, narrow band imaging, and chromoscopy. Once

* Corresponding author.
** Corresponding author.
*** Corresponding author.
E-mail addresses: wellington.pham@vanderbilt.edu (W. Pham), hiro_nakase@sapmed.ac.jp (H. Nakase), sakuma@pharm.setsunan.ac.jp (S. Sakuma).
[1] Present address: Center Director's Strategic Program, RIKEN Center for Life Science Technologies (CLST), Kobe 650-0047, Japan.
[2] Present address: Department of Gastroenterological Medicine, Iseikai Hospital, Osaka 553-0022, Japan.

https://doi.org/10.1016/j.ejpb.2019.01.007
Received 20 July 2018; Received in revised form 21 December 2018; Accepted 8 January 2019
Available online 09 January 2019
0939-6411/

identified, the decision to remove the mucosal growth or polyp is based on size [6]. It has been reported that the sensitivity and specificity of colonoscopy for colorectal adenomas of a size larger than 10 mm are as high as 95% and 90%, respectively [7]. The sensitivity and tumor size are closely linked; the former significantly reduces when the latter is too small. For example, it has been reported that the sensitivity of detecting colorectal cancer with a size of < 5 mm is merely 75% [7,8]. It is still a challenge to detect colorectal cancer in the early stage using the current state-of-the-art colonoscopy. Enhancement of the detection limit of colonoscopy through topical application of non-specific contrasting dyes, a procedure called chromoscopy, has certainly gained attention. In fact, Brown et al. recently reported that the rate of detection of small polyps reached 90% [9], and none of the studies described in that work reported any adverse effects related to the use of the dyes.

Over a decade ago, the incorporation of narrow band imaging in colonoscopy allowed the detailed inspection of vascular and mucosal patterns, which made it possible to predict histology during real-time endoscopy [10]. However, unfortunately, it appears that there is no significant difference between a conventional white-light colonoscopy and narrow band imaging regarding the detection of polyps, adenomas, or hyperplastic polyps by meta-analysis [11]. Particularly, small and flat adenocarcinomas can still elude detection by conventional colonoscopy and the rough mucosal surface only exacerbates the problem [12]. Lately, cancer epigenetics, especially in aberrant DNA methylation, has been vigorously investigated. For instance, it has been reported that sensitivity and specificity for diagnosis of colorectal cancer via methylated DNA of secreted frizzled related proteins in fecal DNA are 77–90% and 77%, respectively [13]. However, these tests do not provide information on the location of colorectal cancer even if they exhibit excellent sensitivity and specificity. Patients have to undergo colonoscopy eventually when they receive a positive result from such tests.

One of the ideal surface biomarkers suitable for integration with colonoscopy is the Thomsen-Friedenreich (TF) antigen. This cancer-related carbohydrate (Galβ1-3GalNAc-α-O-Ser/Thr) is overexpressed on the mucosal surface in colorectal cancer [14–19], partly because the TF antigen is co-expressed with MUC1, a transmembrane protein that is O-glycosylated on the apical surface of epithelial cells lining the mucosal surface of the colon [14,20]. Reduced/aberrant glycosylation of MUC1 is overexpressed in colorectal cancer and has gained remarkable attention as an oncogenic marker [21]. Here, we developed the nanobeacon, which is polystyrene-based nanospheres coated with peanut agglutinin (PNA) on their surface as biorecognition moieties for the TF antigen, to image the antigen-associated colorectal cancer [22]. The fluorescent signal of the nanobeacon emanates from coumarin 6 that is encapsulated into the nanosphere core. Furthermore, an extremely thin layer of poly(N-vinylacetamide) (PNVA) was fabricated on the outer surface of the nanobeacon to reduce non-specific interaction with the gastrointestinal mucosa as reported previously [23–26]. We have previously tested and confirmed the sensitivity and specificity of the nanobeacon for detection of colorectal cancer in imaging based on human colorectal cancer cells [24] and orthotopic rodent models [12,26,27] as well as ex vivo optical imaging using freshly biopsied specimens from clinical surgery [28]. The diagnosis of colorectal cancer by the nanobeacon accompanies identification of the cancer location under endoscopic observation. This point is advantageous to the nanobeacon when compared with other diagnostic strategies.

The rat study in accordance with Good Laboratory Practice regulations has already demonstrated that the nanobeacon can be developed as a safe diagnostic agent for colonoscopy applications [29], although additional toxicity studies such as uptake of the nanobeacon by M cells on Peyer's patches may be required. In order to bring the technology one step closer to clinical trials, the present study was performed with 2 objectives: (i) validation of diagnostic capabilities of the nanobeacon for detection of colorectal cancer and (ii) evaluation for its potential use in the clinic. To achieve the former objective, we prepared 20 production batches of the nanobeacon with fine-tuned characteristics and tested their interactions with 66 normal and 69 tumor tissues removed from the colon of nude mice with or without orthotopically implanted human colorectal cancer; this was followed by quantification of optical images and estimation of the sensitivity and specificity of the nanobeacon through analysis using the receiver operating characteristic (ROC) curves. For the latter objective, we quantified optical images of the nanobeacon-treated normal and tumor tissues on the mucosa biopsied endoscopically from 11 patients with colorectal tumors and evaluated a likelihood for diagnosis of colorectal cancer by intracolonically administered nanobeacon through a difference in fluorescence illumination between both tissues.

2. Materials and methods

2.1. Materials

N-Vinylacetamide (NVA) monomers were obtained from Showa Denko Co. (Tokyo, Japan). Styrene and *t*-butyl methacrylate (BMA) were purchased from Wako Pure Chemical Industries Co., Ltd. (Osaka, Japan). Coumarin 6 and PNA were obtained from Tokyo Chemical Industry Co., Ltd. (Tokyo, Japan) and Sigma-Aldrich (St. Louis, MO), respectively. All chemicals were reagent-grade commercial products and were used without further purification, except for styrene that was purified by distillation.

HT-29 cells, which are a human colorectal adenocarcinoma cell line, were purchased from Dainippon–Sumitomo Pharma Biomedical Co. Ltd. (Osaka, Japan). McCoy's 5A Medium, Modified (with sodium bicarbonate, without L-glutamine), penicillin-streptomycin (10,000 U/mL penicillin and 10 mg/mL streptomycin), nonessential amino acids (10 mM), trypsin-ethylenediaminetetraacetic acid (EDTA) (0.25% trypsin and 1 mM EDTA), and fetal bovine serum (FBS) were obtained from Thermo Fisher Scientific (Waltham, MA). L-Glutamine (200 mM) was obtained from Wako Pure Chemical Industries Co., Ltd. Dulbecco's Phosphate Buffered Saline (PBS with $CaCl_2$ and $MaCl_2$, PBS (+)) and Dulbecco's Phosphate Buffered Saline, Modified (PBS without the divalent ions, PBS (−)) were obtained from Sigma-Aldrich.

2.2. Chemical synthesis and characterization of the nanobeacon

The nanobeacon was prepared in the same manner as previously described [25]. Briefly, NVA and BMA monomers were radically polymerized, respectively, in the presence of 2-mercaptoethanol. The polymerized form of the latter was subsequently hydrolyzed in the presence of hydroquinone. The resulting hydroxyl group-terminated poly(N-vinylacetamide) (PNVA) and poly(methacrylic acid) (PMAA) with terminal vinylbenzyl groups were copolymerized with styrene in an ethanol-water mixture containing 2,2′-azobisisobutyronitrile and coumarin 6 to provide fluorescent nanospheres whose surfaces were covered with PNVA and PMAA chains. The encapsulation of coumarin 6 into the nanosphere core occurred concomitantly during the process of copolymerization. Finally, PNA molecules were immobilized on the surface of the fluorescent nanospheres through the coupling to PMAA chains to provide the nanobeacon. Twenty production batches of the nanobeacon with fine-tuned characteristics were prepared in this study.

The nanobeacon was characterized using the procedures described in our previous studies [26,27,29,30]. Briefly, weight-average and number-average molecular weights (Mw and Mn) of PNVA and PMAA were determined by gel permeation chromatography (GPC). The particle size, aggregation fraction, and zeta potential were measured in PBS (+) by electrophoretic light-scattering spectrophotometry. Fluorescence intensities and immobilized amounts of PNA were measured by fluorescence spectrophotometry and the ninhydrin method, respectively. Data of physicochemical properties of the nanobeacon were expressed as mean ± 95% confidence interval (95% CI).

2.3. Validation of diagnostic capabilities of the nanobeacon for detection of colorectal tumors in orthotopic mouse models of colorectal cancer

2.3.1. Preparation of mouse tissues with or without tumors

2.3.1.1. Cell culture. HT-29 cells were cultured in McCoy's 5A Medium, Modified supplemented with penicillin (50 U/mL), streptomycin (50 μg/mL), L-glutamine (1.5 mM), and FBS (10%, v/v) at 37 °C in a humidified atmosphere of 95% O_2/5% CO_2. For the below-mentioned injection to mice, the cells were harvested from a cell culture flask and then suspended in PBS (−) at a concentration of 1×10^6 cells/0.01 mL.

2.3.1.2. Mouse experiments. Animal studies were approved by the Ethical Review Committee of Setsunan University. An orthotopic mouse model of colorectal cancer was prepared using the same procedures as described in our previous report [12]. Briefly, a sharp incision in the midline of the abdomen of isoflurane-anesthetized nude mice (BALB/c nu/nu, female, 7 weeks) was made to reveal the descending colon. Then, the cell suspension (0.01 mL) was injected into the colonic serosa of the mouse. The process was repeated at several sites of the colon before wound closure. The progress of tumor development in this model was recognized, when the implanted cancer cells started to grow from the serosa and invaded the mucosal side of the intestine. Generally, if that occurred, bloody stools were observed from 6 to 7 weeks after cell implantation as an index of tumor invasion.

For the below-mentioned ex vivo imaging, mice were sacrificed with excessive isoflurane anesthesia and the whole colon was removed followed by a longitudinal dissection. After the colon was washed with PBS (−), extra volumes of tumors on the serosal surface were carefully removed. Small pieces of tissues bearing tumors on the mucosal surface were collected using a 3-mm size tissue puncher (Sigma-Aldrich). The same procedures were performed for normal nude mice without the cancer cell implantation to obtain small pieces of normal (control) tissues. Freshly prepared tissues were preserved in ice-cooled PBS (−) for a maximum of 3 h before every imaging session. Overall, in this study, 69 colonic tissues bearing tumors derived from human colorectal cancer cells and 66 normal tissues were prepared.

2.3.2. Optical imaging of mouse tissues treated with the nanobeacon

The optical imaging was performed under experimental protocols established in our latest publication [28]. In general, mouse tissues were treated with the nanobeacon dispersed in PBS (+) at a concentration of 10 mg/mL (0.1 mL) on ice for 2 min. The treatment was followed by a brief wash of tissues with ice-cooled PBS (+) (1.5 mL) for 30 sec to remove any excess amount of the nanobeacon that interacted non-specifically with them. After the washing process was repeated 4 times, tissues were observed with a fluorescence microscope (IX71-22FL/PH, Olympus Co., Ltd., Tokyo, Japan, excitation: 470–495 nm, emission: 510–550 nm). Tissue images were captured with a CCD camera (DP71, Olympus Co., Ltd.) equipped to the fluorescence microscope with an exposure time of 1/30 and 1/60 sec for fluorescence and white light observation, respectively (operation software: Lumina Vision (Mitani Co., Fukui, Japan)).

2.3.3. Validation of diagnostic capabilities of the nanobeacon

2.3.3.1. Quantification of optical images. The intensities of the nanobeacon-emitted fluorescent signal in the optical images of tissues captured as described in Section 2.3.2. were quantified and characterized using an imaging analysis software (WinROOF2013, Mitani Co.). The threshold was set to 35 in the software in order to remove background signals and draw tissue edges in outline. Mean fluorescence intensities (MFIs) inside the outline were calculated through quantification of fluorescence in each image.

2.3.3.2. Calculation of parameters that estimate diagnostic capabilities. A couple of parameters were used to validate diagnostic capabilities of the nanobeacon for detection of colorectal tumors. One was sensitivity, which is defined as a parameter that categorizes cancer tissues as cancer. The other was specificity, which is defined as a parameter that categorizes normal tissues as normal. The sensitivity and specificity are also designated as true positive and true negative values, respectively. Several cut-off points, which were based on the average and standard deviation (SD) of MFIs of the nanobeacon-treated normal tissues, were set as a criterion to provide the sensitivity and specificity. Here, average + 1 × SD, 2 × SD, 3 × SD, and 4 × SD were used. The diagnosis was performed for all the optical images captured as described in Section 2.3.2. The rate of true positives was calculated as the percentage of the number of the nanobeacon-treated cancer tissues whose MFI was more than the criterion for the total number of cancer tissues (100 × sensitivity). The rate of true negatives was calculated as the percentage of the number of the nanobeacon-treated normal tissues whose MFI was less than the criterion for the total number of the normal tissues (100 × specificity). Rates of false positives and false negatives were also calculated as the percentage of the number of the nanobeacon-treated normal tissues whose MFI was more than the criterion for the total number of normal tissues (100 × (1 − specificity)) and that of the number of the nanobeacon-treated cancer tissues whose MFI was less than the criterion for the total number of cancer tissues (100 × (1 − sensitivity)), respectively.

2.3.3.3. Preparation of the receiver operating characteristic (ROC) curves. The ROC curves are generally used to validate the quality of a diagnostic agent through determination of the criterion that exhibits the best combination of the high rate of true positives (high sensitivity) and the low rate of false positives (low 1 − specificity). This data was prepared using the respective values obtained in Section 2.3.3.2. The area under the ROC curve (AUC_{ROC}) was also calculated.

2.4. Evaluation for the potential use of the nanobeacon in the clinic under the cooperation of human volunteers

2.4.1. Endoscopic biopsy of human tissues

Clinical studies were approved by the Ethical Review Committee for Medical and Health Research Involving Human Subjects of Setsunan University and the Institutional Review Board of Osakafu Saiseikai Nakatsu Hospital. Eleven patients with colorectal tumors participated in the studies. Pathological tissues on the large intestinal mucosa that were diagnosed endoscopically as tumor by physicians were biopsied through standard procedures of colonoscopy in the hospital (ca. 3 mm × 3 mm, more than 2 tissues/patient). One of the biopsied tissues was transferred for histological evaluation as described in Section 2.4.4. Non-pathological tissues diagnosed as normal under the endoscopic observation were simultaneously collected from the same patient (1 tissue/patient). Freshly biopsied tissues were preserved in ice-cooled PBS (−) for a maximum of 3 h before every imaging session.

2.4.2. Optical imaging of human tissues treated with the nanobeacon

The optical imaging was performed as done for mouse tissues in Section 2.3.2.

2.4.3. Evaluation for the potential use of the nanobeacon in the clinic

2.4.3.1. Quantification of optical images. MFIs of the nanobeacon-treated human tissues were calculated, as done for mouse tissues in Section 2.3.3.1.

Another quantification was performed for human tissues. The percentage of areas with fluorescence intensities that were larger than predetermined thresholds was calculated. In the imaging analysis software, 35 was used as the minimum threshold. The percentage was calculated in the threshold range of 35–70.

2.4.3.2. Estimation of diagnostic performance of the nanobeacon in the clinic. MFIs of the nanobeacon-treated tumor (pathological) tissues were compared with those of the nanobeacon-treated normal (non-

pathological) ones using the values obtained in Section 2.4.3.1. Comparison of the area percentage was also performed.

2.4.4. Histological evaluation of biopsied human tissues

Endoscopic biopsy of pathological tissues was followed by a histological evaluation by pathologists in order to provide a definitive diagnosis, as done commonly for the diagnosis and treatment of colorectal tumors.

2.5. Statistical analysis

Unpaired Student's *t*-test and paired test were used for statistical analysis of mouse and human studies, respectively, and $p < 0.05$ was considered statistically significant.

3. Results and discussion

3.1. The reproducibility of the nanobeacon

Characteristics of the nanobeacon were fine-tuned using the optimized chemistry. Average data with 95% CI of its 20 production batches summarized in Table 1 demonstrated the reproducibility of the nanobeacon. The particle size of the nanobeacon was 315 ± 41 nm. Our calculation supported that each particle of the nanobeacon possessed 200–300 PNA molecules, while coumarin 6 constituted approximately 0.05% of the overall weight of the nanobeacon. The particle size and zeta potential were measured in neutral solution whose pH corresponded to that of the administration site (the large intestine) of the nanobeacon. The characteristics were almost identical to those described previously [26,27,29–31]. Our past study on the stability of the nanobeacon indicated that the characteristics would be constant through the current research [29]. All batches were used for mouse studies. Among them, 4 batches, whose individual data are shown in Table 1, were provided for human studies. We have separately established in vitro methods for estimation of biological activities of the nanobeacon, such as hemagglutination using Galβ1-3GalNAc-expressing red blood cells and biorecognition using the TF antigen-expressing human colorectal cancer cells [24,30]. These tests were not performed because validation of diagnostic capabilities of the nanobeacon for detection of colorectal cancer using rodent and human tissues were planned in the present study, as mentioned below.

3.2. Validation of diagnostic capabilities of the nanobeacon for detection of colorectal tumors in orthotopic mouse models of colorectal cancer

Fig. 1A shows the representative fluorescence images of normal and cancer tissues treated with the nanobeacon. Cancer tissues obtained from cancer cells-implanted nude mice were clearly illuminated by the nanobeacon as compared to normal tissues obtained from implantation-free nude mice, irrespective of the production batch of the nanobeacon. As shown in Fig. 1B, the average of the MFIs for 69 nanobeacon-treated cancer tissues was significantly higher than that for 66 nanobeacon-treated normal tissues. Furthermore, approximately 3-fold signal enhancement was observed in the former as compared to the latter counterpart. This data strongly supported that the nanobeacon was very specific for detection of colorectal cancer. The current observation was consistent with our previously reported results [23,28]. The difference in intensities of the nanobeacon-emitted fluorescence between both the tissues was presumably due to high expression of the TF antigen in cancer tissues that was recognized by PNA on the nanosphere surface.

We subsequently validated diagnostic capabilities of the nanobeacon for detection of HT-29 cells-derived colorectal tumors in nude mice. As shown in Table 2, criteria, which were based on the average and standard deviation of MFIs of the nanobeacon-treated normal tissues, affected the sensitivity and specificity of the nanobeacon. The sensitivity (the rate of true positives) decreased with an increase in the value of criteria. This was due to the identification of the nanobeacon-treated cancer tissues with a relatively low MFI as normal, indicating that the rate of false negatives increased. On the other hand, the specificity (the rate of true negatives) decreased with a decrease in the value of criteria. This was due to the identification of the nanobeacon-treated normal tissues with a relatively high MFI as cancer, indicating that the rate of false positives increased. Fig. 2 shows the ROC curve constructed through a plot of each combination of sensitivity and specificity in Table 2. Theoretically, plots in ROC curves and AUC_{ROC} approach a top-left corner of the figure and a value of 1, respectively, as diagnostic performance becomes better. As shown in Fig. 2 and Table 2, the best combination of a high rate of true positives (91%) and a low rate of false positives (5%) was observed when the average + 2 × SD was set as a criterion. It was concomitant with the best combination of a high rate of true negatives (95%) and a low rate of false negatives (9%). As shown in Table 3, AUC_{ROC} was calculated to be 0.96.

3.3. Evaluation for the potential use of the nanobeacon in the clinic under the cooperation of human volunteers

Conventional colonoscopy is not generally suitable for flat and depressed neoplasms [32,33,34,35]. Patients with chronic inflammatory bowel disease face increased risk of developing malignancy due to undetected dysplastic lesions [33,36]. The nanobeacon should be primarily developed in the clinic as a tool that solves such unmet needs in high-risk patients. Under colonoscopic observation in such patients,

Table 1
Characteristics of the nanobeacon used in this research.

Characteristics	For mouse studies	For human studies			
	(Mean ± 95% CI, n = 20)	Lot A	Lot B	Lot C	Lot D
The molecular weight of PNVA (Mw/Mn)	19749 ± 513/6165 ± 52	Mixture[e]	19900/6200	19900/6200	19900/6200
The molecular weight of PMAA (Mw/Mn)	36578 ± 1797/27479 ± 1106	8300/4930	8300/4930	29900/23900	29900/23900
Particle size (nm)[a]	315 ± 41	470 ± 500	380 ± 320	290 ± 220	180 ± 130
Fluorescent intensity[b]	27825 ± 3375	51,000	43,000	46,000	20,000
Immobilized PNA (μg/mg)[c]	3.1 ± 0.6	3.6	2.4	2.9	1.37
Zeta potential (mV)	−28.1 ± 1.0	−29.3	−29.6	−27.9	−26.9
Aggregation fraction (%)[d]	3.3. ± 3.7	0	0	0	0

[a] wt-average diameter.
[b] Fluorescence intensity of the nanobeacon dispersed in PBS (+) at a concentration of 1 mg/mL.
[c] Amount of PNA immobilized in the nanobeacon (μg/mg).
[d] Percentage of scattering intensities derived from the aggregated nanobeacon whose diameter was larger than 1 μm for the total scattering intensities. The distribution of scattering intensities was used for the calculation.
[e] Three production batches of PNVA with a different molecular weight (Mw/Mn: 15080/5990, 19900/6200, and 21700/5700) were mixed at a weight ratio of 1:1:1.

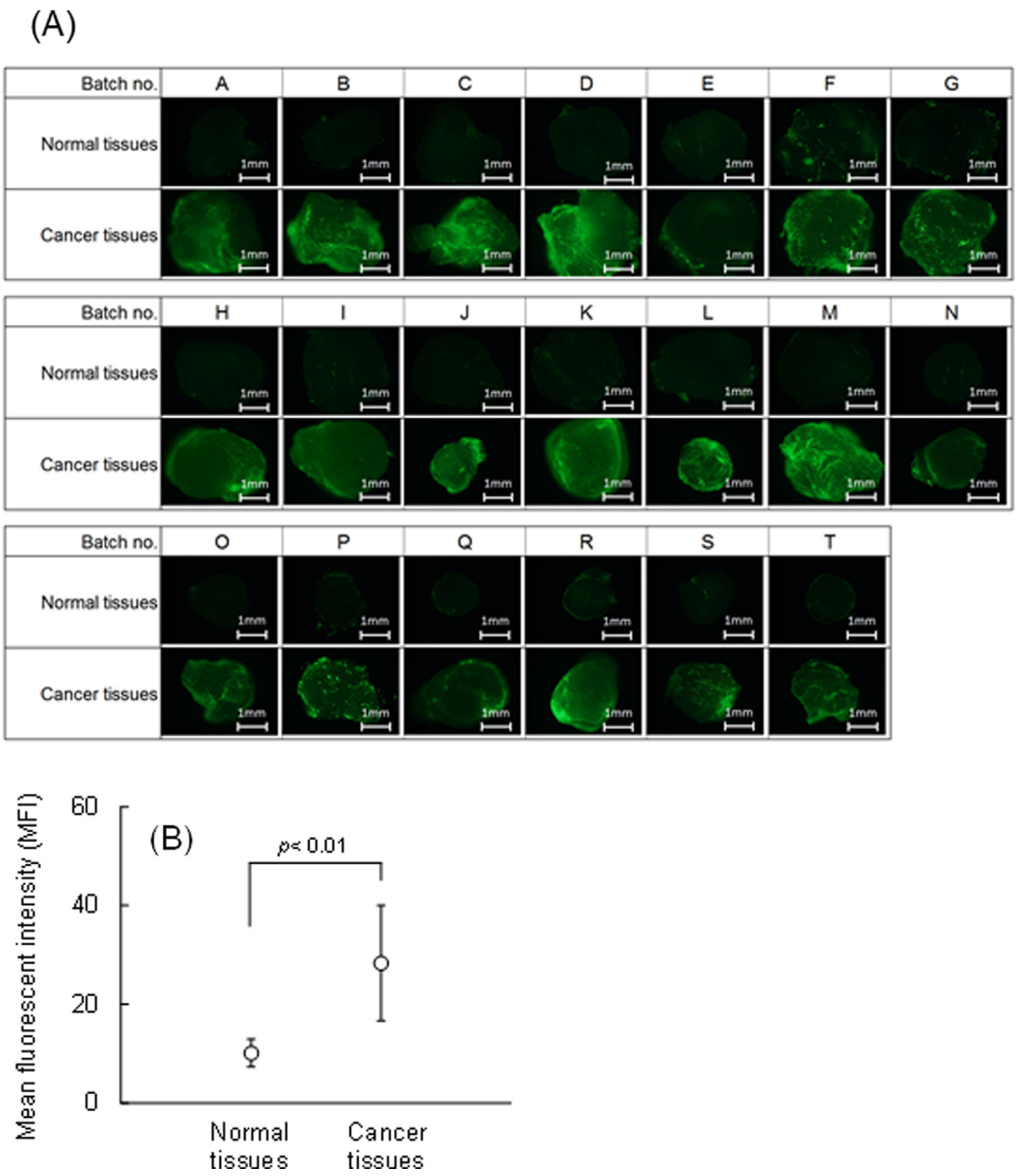

Fig. 1. The representative fluorescence images (A) and mean fluorescence intensities (MFI) (B) of normal and cancer tissues in mice treated with the nanobeacon. Human colorectal cancer cells (HT-29 cells) were orthotopically implanted in the serosa of the colon in nude mice. The mice were sacrificed after the mucosal invasion of HT-29 cells-derived tumors, and the colon was then divided into small pieces to obtain cancer tissues. Small pieces of normal tissues were separately prepared from the colon of normal nude mice in a manner similar to that described above. Incubation of normal and cancer tissues with the nanobeacon dispersed in PBS (+) was followed by a brief wash with the nanobeacon-free PBS. The nanobeacon-treated tissues were observed with a fluorescence microscope (excitation: 470–495 nm, emission: 510–550 nm, exposure time: 1/30 sec). The MFI was calculated through an imaging analysis software-driven quantification for fluorescence images of tissues. Values of normal and cancer tissues represent average ± SD of 66 and 69 images, respectively.

intracolonic administration of the nanobeacon is followed by a washout of the bulk amount of the nanobeacon that interacts non-specifically with normal tissues. Following this, downstream diagnostic steps are based on detection of significant fluorescence contrast between normal and pathological tissues, biopsy of the nanobeacon-illuminated pathological tissues, and their histological evaluation.

The mouse study in the previous section demonstrated that the nanobeacon recognized cancer tissues with high sensitivity and specificity. We expect that the same holds true when the nanobeacon is applied to colorectal cancer in humans. The present clinical ex vivo imaging study aimed to compare the nanobeacon-emitted fluorescence in tumor tissues with that in normal tissues. Eleven patients with colorectal tumors kindly donated normal (non-pathological) tissues on the large intestinal mucosa along with tumor (pathological) tissues, which were then graded histologically as shown in Table 4. Tumor tissues biopsied from patients numbered 5 and 8 were diagnosed as adenomas and the tissues from the remaining 9 patients were diagnosed as cancer. Fig. 3 shows MFIs of normal and tumor tissues treated with the nanobeacon. The statistical analysis is summarized in Table 5. MFIs of tumor tissues were significantly higher than those of the corresponding normal tissues. However, its inversed relation with a small difference was observed in tissues obtained from patients numbered 2 and 8, who

Table 2
Sensitivity and specificity of the nanobeacon for detection of tumors derived from human colorectal cancer cells (HT-29 cells) implanted orthotopically in nude mice.

Criteria[a]	Sensitivity	Specificity	Distance[b]
Average	0.97	0.65	0.35
Average + 1 × SD	0.96	0.83	0.18
Average + 2 × SD	0.91	0.95	0.10
Average + 3 × SD	0.77	0.97	0.23
Average + 4 × SD	0.68	1	0.32

[a] Criteria were based on the average and standard deviation (SD) of mean fluorescence intensities of all normal tissues treated with the nanobeacon (n = 66).

[b] Distance between each plot and top-left corner (a value of x-axis: 0, a value of y-axis: 1) in the ROC curve.

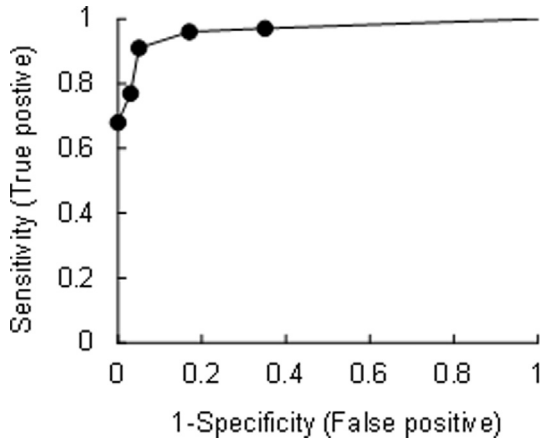

Fig. 2. The receiver operating characteristic (ROC) curve for validation of diagnostic capabilities of the nanobeacon for detection of tumors derived from human colorectal cancer cells (HT-29 cells) implanted orthotopically in nude mice. The curve was constructed by plotting each combination of sensitivity and specificity in Table 2 that were calculated using several criteria based on the average and standard deviation of mean fluorescence intensities of the nanobeacon-treated normal tissues in mice.

Table 3
The area under the receiver operating characteristics curves (AUC_{ROC}) calculated for the nanobeacon-treated mouse tissues on the basis of methodology with a different aspect.

	Analysis using MFI	Analysis using a threshold of 70
AUC_{ROC}	0.96	0.86

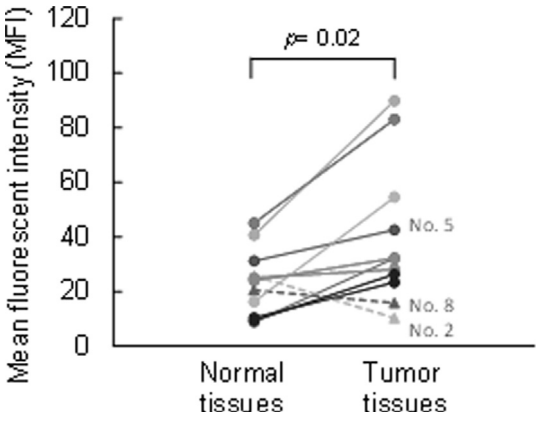

Fig. 3. Mean fluorescence intensities (MFI) of normal (non-pathological) and tumor (pathological) tissues in humans treated with the nanobeacon. Tumor tissues on the large intestinal mucosa that were diagnosed endoscopically as cancer by physicians were biopsied from 11 patients with colorectal tumors through standard procedures of colonoscopy. Normal tissues were simultaneously collected from the same patients. Incubation of normal and tumor tissues with the nanobeacon dispersed in PBS (+) was followed by a brief wash with the nanobeacon-free PBS. The nanobeacon-treated tissues were observed with a fluorescence microscope (excitation: 470–495 nm, emission: 510–550 nm, exposure time: 1/30 sec). The MFI was calculated through an imaging analysis software-driven quantification for fluorescence images of tissues. The MFI of tumor tissues was plotted against the corresponding MFI of normal tissues.

suffered from early cancer and adenoma, respectively. The magnitude of MFIs of tumor tissues in both patients also indicated that interactions between the tissues and the nanobeacon were weak as compared to the remaining cases.

Our latest study demonstrated that there was a unique pattern of fluorescence intensities in illuminations in pathological and non-pathological tissues by the nanobeacon; it was utilized as a quantitative algorithm to differentiate normal tissues from cancer ones [28]. That work also indicated that tumors would be distinguished from normal tissues through comparison of the areas with fluorescence intensities that were larger than the predetermined thresholds. This comparison was temporarily performed for the nanobeacon-treated tissues with the unexpected pattern of fluorescence intensities (tumor tissues < normal tissues) biopsied from patients numbered 2 and 8. The imaging analysis software was used to find an adequate threshold. As shown in Fig. 4, when 35, which is the number in the software that removes background signals and draws tissue edges in outline, was set as a threshold, the percentage of the areas with fluorescence intensities above the threshold in the tumor tissue was less than that in the corresponding normal one in both patients. This magnitude correlation was same as that observed for the analysis using MFIs (Fig. 3). The percentage

Table 4
Histological evaluation of human tissues biopsied as tumor (pathological) under colonoscopic observation by physicians.

Patient no.	Region	Tumor condition	Morphology	Preoperative staging	The nanobeacon used (Batch no.)
1	Ascending colon	Advanced cancer	2	IV	B
2	Sigmoid colon	Early cancer	Isp	–[a]	B
3	Sigmoid colon	Early cancer	IIa	–[a]	B
4	Ascending colon	Advanced cancer	2	IIIa	A
5	Descending colon	Tubular adenoma	Is	–[a]	C
6	Sigmoid colon	Advanced cancer	2	IV	C
7	Sigmoid colon	Adenocarcinoma	2	II	C
8	Sigmoid colon	Adenoma	Isp	–[a]	C
9	Sigmoid colon	Advanced cancer	2	II	C
10	Rectum	Advanced cancer	3	IIIa	C
11	Ascending colon	Advanced cancer	1	I	D

[a] Not classified because tumor condition was early cancer or adenoma.

Table 5
Statistical analysis of fluorescence intensities in the nanobeacon-treated normal and tumor tissues biopsied from patients with colorectal tumors (n = 11) calculated on the basis of methodology with a different aspect.

Tissue type	Analysis using MFI			Analysis using a threshold of 70		
	Average ± SD	CV%	*p*	Average ± SD	CV%	*p*
Normal (non-pathological)	23.38 ± 12.15	51.97	0.02	1.99 ± 2.70	135.68	0.06
Tumor (pathological)	39.95 ± 25.97	65.01		18.11 ± 28.06	154.94	

almost linearly reduced with an elevation of the threshold. The unexpected fluorescence pattern was constantly observed in tissues biopsied from the patient with adenoma (patient no. 8) even when the percentage approached 0 (Fig. 4B). On the other hand, the fluorescence pattern in tissues biopsied from the patient with early cancer (patient no. 2) was normalized (tumor tissues > normal tissues), when the threshold exceeded 60 (Fig. 4A).

Since the number of patients with the expected fluorescence pattern elevated through this analysis, the area percentage with a threshold of 70 was similarly calculated for the remaining 9 patients. As shown in Fig. 5, the area percentage in tumor tissues biopsied from a total of 10 patients was larger than that in the corresponding normal tissues. However, the improved diagnostic capabilities were concomitant with an insignificant difference in fluorescence intensities between normal and tumor tissues, presumably due to an expanded variation of intensities (Table 5). Regarding with the analysis using a threshold of 70, retrospective calculation of AUC_{ROC} was performed on mouse data (Table 3). Comparison between both values in Table 3 revealed that the analysis using MFIs was superior to that using the threshold. Results indicated that the former analysis should be applied prior to the latter one.

We finally discussed a likelihood for diagnosis of colorectal tumors by the nanobeacon in humans. Histological evaluation revealed that cancer and adenoma grew on the mucosa of the large intestine in 9 and 2 patients, respectively (Table 4). The nanobeacon detected pathological changes in mucosal tissues biopsied from 8 patients with colorectal cancer with the tissue images being primarily analyzed using MFIs, indicating that the probability of cancer detection was 89%. The probability reached 100% through the secondary analysis using the percentage of areas with fluorescence intensities above 70 as a threshold (Figs. 3 and 4A). On the other hand, the nanobeacon failed to detect pathological changes in mucosal tissues biopsied from patients with adenoma with a probability of 50% when the analysis using MFIs was performed. This low probability was constant, irrespective of the aspect of methodologies (Figs. 3 and 4B). It seemed that the diagnostic capability of the nanobeacon for adenoma was inferior to that for

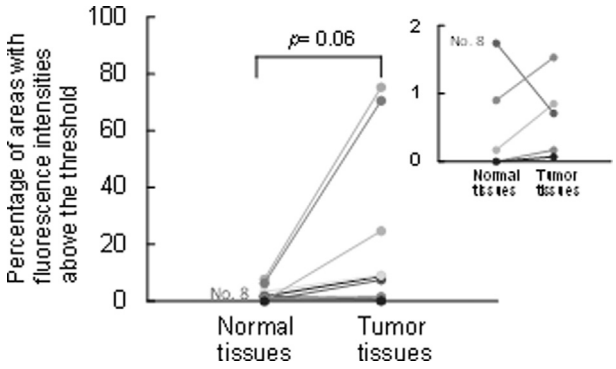

Fig. 5. The percentage of areas with fluorescence intensities that were larger than the threshold of 70 in normal (non-pathological) and tumor (pathological) tissues biopsied from 11 patients with colorectal tumors. Normal and tumor tissues on the large intestinal mucosa were biopsied from the same patients under endoscopic observation. Their incubation with the nanobeacon dispersed in PBS (+) was followed by a brief wash with the nanobeacon-free PBS. The nanobeacon-treated tissues were observed with a fluorescence microscope (excitation: 470–495 nm, emission: 510–550 nm, exposure time: 1/30 sec).

cancer. We expect that the nanobeacon enables to diagnose colorectal cancer through quantitative analysis of the mucosal surface illuminated by the intracolonically administered nanobeacon.

We concluded that there was a reasonable likelihood for a diagnosis of colorectal cancer by the nanobeacon. The number of patients with adenoma, who participated in the study, was so small that low probability of adenoma detection may not always deny diagnostic capabilities of the nanobeacon for adenoma. Boland et al. [15] reported that the PNA reactivity depended on the neoplastic progression of the colonic mucosa. The reactivity to an adenoma with low-grade dysplasia was inferior to that to an adenoma with high-grade dysplasia. The reactivity further increased when adenoma was substituted with carcinoma. Baldus et al. [14] also reported that a similar correlation for adenoma was observed in human tissues. Such reports indicate that the

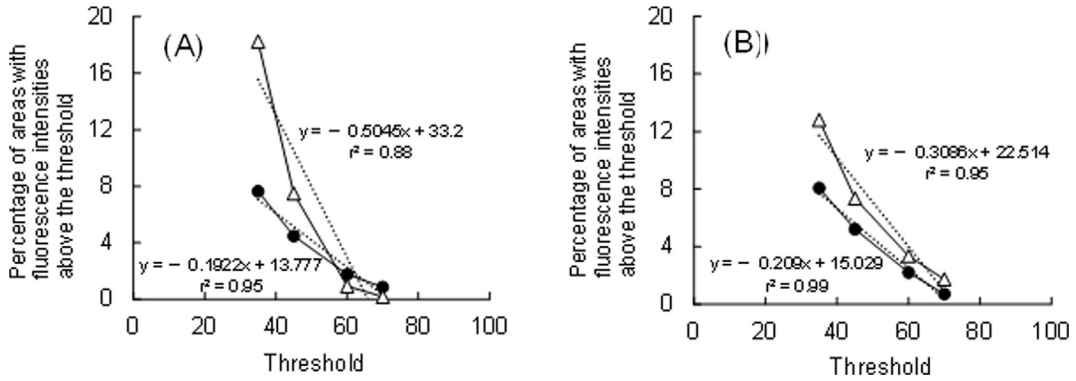

Fig. 4. The percentage of the areas with fluorescence intensities that were larger than the predetermined thresholds in normal (non-pathological) (△) and tumor (pathological) tissues (●) biopsied from patients numbered 2 (A) and 8 (B). Normal and tumor tissues on the large intestinal mucosa were biopsied from the same patients under the endoscopic observation. Their incubation with the nanobeacon dispersed in PBS (+) was followed by a brief wash with the nanobeacon-free PBS. The nanobeacon-treated tissues were then observed with a fluorescence microscope (excitation: 470–495 nm, emission: 510–550 nm, exposure time: 1/30 sec). An imaging analysis software was used for setting of thresholds.

expression level of the TF antigen elevates through the neoplastic progression. We expect that sensitivity of the nanobeacon to adenoma is improved through an elevation of the amount of PNA immobilized on the nanosphere surface. However, we consider that the diagnostic capabilities of the nanobeacon for adenoma are not a prerequisite for its clinical use because current technologies, including colonoscopy, almost enable physicians to detect adenoma without a significant oversight [7]. We should, therefore, focus on unmet needs in the current colonoscopy technologies.

4. Conclusions

In the present study, diagnostic capabilities of the nanobeacon (peanut agglutinin-immobilized fluorescent nanospheres) for detection of colorectal cancer were validated in orthotopic mouse models of colorectal cancer. Ex vivo imaging studies on normal and cancer tissues collected from the mice demonstrated that the nanobeacon detected colorectal cancer with excellent capabilities whose rates of true and false positives were 91% and 5%, respectively. The potential use of the nanobeacon in the clinic was also evaluated using mucosal tissues of the large intestine biopsied endoscopically from 11 patients with colorectal tumors. Histological evaluation revealed that 9 patients suffered from cancer and the remaining ones had adenoma. Mean fluorescence intensities (MFIs) of tumor tissues treated with the nanobeacon were significantly higher than those of the corresponding normal tissues. Correlation of magnitude relation of the intensity in individuals was observed in cancer patients with a high probability (89%); the probability reached 100% through additional analysis using the percentage of areas with fluorescence intensities above predetermined thresholds in the nanobeacon-treated tissues. It seemed that the diagnostic capability of the nanobeacon was inferior for adenoma than for cancer. We expect that the nanobeacon enables physicians to diagnose colorectal cancer through quantitative analysis of the illumination of the mucosal surface following intracolonically administered nanobeacon.

Acknowledgements

This work was partially funded by NIH grants [R01CA1160700] (W.P.) and VICC Cancer Center Support Grant (W.P.). The authors would like to extend their appreciation to Dr. Hideto Senzaki, M.D., Ph.D. and Ms. Yoshimi Miyagi, M.D., who are pathologists at the Division of Pathology, Osakafu Saiseikai Nakatsu Hospital for performing histological evaluation of biopsied human tissues.

References

[1] R.L. Siegel, K.D. Miller, A. Jermal, Cancer statistics 2017, CA Cancer J. Clin. 67 (2017) 7–30.
[2] Cancer statistics in Japan, Foundation for promotion of cancer research, 2015, pp. 1–128.
[3] A. Takamori, K. Nakamura, S. Ukawa, E. Okada, M. Hirata, A. Nagai, K. Matsuda, Y. Kamatani, K. Muto, Y. Kiyohara, Z. Yamagata, T. Ninomiya, M. Kubo, Y. Nakamura, BioBank Japan Cooperative Hospital Group, Characteristics and prognosis of Japanese colorectal cancer patients: the BioBank Japan Project, J. Epidemiol. 27 (2017) S36–S42.
[4] K. Wada, S. Oba, M. Tsuji, T. Tamura, K. Konishi, Y. Goto, F. Mizuta, S. Koda, A. Hori, S. Tanabashi, S. Matsushita, N. Tokumitsu, C. Nagata, Meat consumption and colorectal cancer risk in Japan: the Takayama study, Cancer Sci. 108 (2017) 1065–1070.
[5] I.A. Issa, M. Noureddine, Colorectal cancer screening: an updated review of the available options, World J. Gastroenterol. 23 (2017) 5086–5096.
[6] A.J. Aldridge, J.N. Simson, Histological assessment of colorectal adenomas by size. Are polyps less than 10 mm in size clinically important? Eur. J. Surg. 167 (2001) 777–781.
[7] A.G. Zauber, I. Lansdrop-Vogrlaar, A.B. Knuden, J. Wilschut, M. Ballegooijen, K.M. Kuntz, Evaluating test strategies for colorectal cancer screening: a decision analysis for the U.S. preventive services task force, Ann. Intern. Med. 149 (2008) 659–669.
[8] G.A.P. Ganepola, J. Nizin, J.R. Rutledge, D.H. Chang, Use of blood-based biomarkers for early diagnosis and surveillance of colorectal cancer, World J. Gastrointestinal Oncol. 6 (2014) 83–97.
[9] S.R. Brown, W. Baraza, S. Din, S. Riley, Chromoscopy versus conventional endoscopy for the detection of polyps in the colon and rectum (review), Cochrane Database Systemat. Rev. 4 (2016) 1–69.
[10] K. Gono, T. Obi, M. Yamaguchi, N. Ohyama, H. Machida, S. Yoshida, Y. Hamamoto, T. Endo, Appearance of enhanced tissue features in narrow-band endoscopic imaging, J. Biomed. Opt. 9 (2004) 568–577.
[11] A. Nagorni, G. Bjelakovic, B. Petrovic, Narrow band imaging versus conventional white light colonoscopy for the detection of colorectal polyps (review), Cochrane Database Systemat. Rev. (2012) 1–3.
[12] T. Kitamura, S. Sakuma, M. Shimosato, H. Higashino, Y. Masaoka, M. Kataoka, S. Yamashita, K. Hiwatari, H. Kumagai, N. Morimoto, S. Koike, E. Tobita, R.M. Hoffman, J.C. Gore, W. Pham, Specificity of lectin-immobilized fluorescent nanospheres for colorectal tumors in a mouse model which better resembles the clinical disease, Contrast Media Mol. Imaging 10 (2015) 135–143.
[13] Y. Okugawa, W.M. Grady, A. Goel, Epigenetic alterations in colorectal cancer: emerging biomarkers, Gastroenterology 149 (2015) 1204–1225.
[14] S.E. Baldus, F.G. Hanisch, G.M. Kotlarek, T.K. Zibes, J. Thiele, J. Isenberg, U.R. Karsten, P. Devine, H.P. Dienes, Coexpression of MUC1 mucin peptide core and the Thomsen-friedenreich antigen in colorectal neoplasms, Cancer 82 (1998) 1019–1027.
[15] C.R. Boland, M. Martin, I. Goldstein, Lectin reactivities as intermediate biomarkers in premalignant colorectal epithelium, J. Cellular Biochem. Suppl. 16G (1992) 103–109.
[16] M.V. Croce, M. Isla-Larrain, M.E. Rabassa, S. Demichelis, A.G. Coulussi, M. Crespo, E. Lacunza, A. Segal-Eiras, Lewis x is highly expressed in normal tissues: a comparative immunohistochemical study and literature revision, Pathology Oncol. Res. 13 (2007) 130–138.
[17] Y. Cao, U.R. Karsten, W. Liebrich, W. Haensch, G.F. Springer, P.M. Schlag, Expression of Thomsen-Friedenreich related antigens in primary and metastatic colorectal carcinomas, Cancer 76 (1995) 1700–1708.
[18] S.H. Itzkowitz, M. Yuan, C.K. Montgomery, T. Kjeldsen, H.K. Takahashi, W.L. Bigbee, Y.S. Kim, Expression of Tn, Sialosyl-Tn, and T antigens in human colon cancer, Cancer Res. 49 (1989) 197–204.
[19] J. Byrd, R. Bresalier, Mucins and mucin binding proteins in colorectal cancer, Cancer Metastasis Rev. 23 (2004) 77–99.
[20] I. Brockhausen, Pathways of O-glycan biosynthesis in cancer cells, Biochim. Biophys. Acta 1473 (1999) 67–95.
[21] S.K. Lau, L.M. Weiss, P.G. Chu, Differential expression of MUC1, MUC1 and MUC5AC in carcinomas of various sites: an immunohistochemical study, Am. J. Clin. Pathol. 122 (2004) 61–69.
[22] S. Sakuma, S. Yamashita, K. Hiwatari, R.M. Hoffman, W. Pham, Lectin-immobilized fluorescent nanospheres for targeting to colorectal cancer from a physicochemical perspective, Curr. Drug Discov. Technol. 8 (2011) 367–378.
[23] H. Kumagai, W. Pham, M. Kataoka, K. Hiwatari, J. McBride, K.J. Wilson, H. Tachikawa, R. Kimura, K. Nakamura, E.H. Liu, J.C. Gore, S. Sakuma, Multifunctional nanobeacon for imaging Thomsen-Friedenreich antigen-associated colorectal cancer, Int. J. Cancer 132 (2013) 2107–2117.
[24] S. Sakuma, T. Yano, Y. Masaoka, M. Kataoka, K. Hiwatari, H. Tachikawa, Y. Shoji, R. Kimura, H. Ma, Z. Yang, L. Tang, R.M. Hoffman, S. Yamashita, In vitro/vivo biorecognition of lectin-immobilized fluorescent nanospheres for human colorectal cancer cells, J. Control. Release 134 (2009) 2–10.
[25] S. Sakuma, J.Y.H. Yu, T. Quang, K. Hiwatari, H. Kumagai, S. Kao, A. Holt, J. Erskind, R. McClure, M. Siuta, T. Kitamura, E. Tobita, S. Koike, K. Wilson, R. Richards-Kortum, E. Liu, K. Washington, R. Omary, J.C. Gore, W. Pham, Fluorescence-based endoscopic imaging of Thomsen-Friedenreich antigen to improve early detection of colorectal cancer, Int. J. Cancer 136 (2015) 1095–1103.
[26] S. Sakuma, T. Yano, Y. Masaoka, M. Kataoka, K. Hiwatari, H. Tachikawa, Y. Shoji, R. Kimura, H. Ma, Z. Yang, L. Tang, R.M. Hoffman, S. Yamashita, Detection of early colorectal cancer imaged with peanut agglutinin-immobilized fluorescent nanosphres having surface poly(N-vinylacetamide) chains, Eur. J. Pharm. Biopharm. 74 (2010) 451–460.
[27] S. Sakuma, H. Higashino, H. Oshitani, Y. Masaoka, M. Kataoka, S. Yamashita, K. Hiwatari, H. Tachikawa, R. Kimura, K. Nakamura, H. Kumagai, J.C. Gore, W. Pham, Essence of affinity and specificity of peanut agglutinin-immobilized fluorescent nanospheres with surface poly(N-vinylacetamide) chains for colorectal cancer, Eur. J. Pharm. Biopharm. 79 (2011) 537–543.
[28] H. Nakase, S. Sakuma, T. Fukuchi, T. Yoshino, K. Mohri, K. Miyata, H. Kumagai, K. Hiwatari, K. Tsubaki, T. Ikejima, E. Tobita, M. Zhu, K.J. Wilson, K. Washington, J.C. Gore, W. Pham, Evaluation of a novel fluorescent nanobeacon for targeted imaging of Thomsen-Friedenreich associated colorectal cancer, Int. J. Nanomed. 12 (2017) 1747–1755.
[29] S. Sakuma, H. Kumagai, M. Shimosato, T. Kitamura, K. Mohri, T. Ikejima, K. Hiwatari, S. Koike, E. Tobita, R. McClure, J.C. Gore, W. Pham, Toxicity studies of coumarin 6-encapsulated polystyrene nanospheres conjugated with peanut agglutinin and poly(N-vinylacetamide) as a colonoscopic imaging agent in rats, Nanomedicine 11 (2015) 1227–1236.
[30] K. Hiwatari, S. Sakuma, K. Iwata, Y. Masaoka, M. Kataoka, H. Tachikawa, Y. Shoji, S. Yamashita, Poly(N-vinylacetamide) chains enhance lectin-induced biorecognition through the reduction of nonspecific interactions with nontargets, Eur. J. Pharm. Biopharm. 70 (2008) 453–461.
[31] S. Sakuma, M. Kataoka, H. Higashino, T. Yano, Y. Masaoka, S. Yamashita, K. Hiwatari, H. Tachikawa, R. Kimura, K. Nakamura, H. Kumagai, J.C. Gore, W. Pham, A potential of peanut agglutinin-immobilized fluorescent nanospheres as a safe candidate of diagnostic drugs for colonoscopy, Eur. J. Pharm. Sci. 42 (2011) 340–347.
[32] S. Kudo, H. Kashida, T. Tamura, E. Kogure, Y. Imai, H. Yamano, A.R. Hart,

Colonoscopic diagnosis and management of nonpolypoid early colorectal cancer, World J. Surg. 24 (2000) 1081–1090.
[33] R. Mayer, W.D. Wong, D.A. Rothenberger, S.M. Goldberg, R.D. Madoff, Colorectal cancer in inflammatory bowel disease: a continuing problem, Dis. Colon Rectum 42 (1999) 343–347.
[34] A. Facciorusso, M. Antonino, M.D. Maso, M. Barone, N. Muscatiello, Non-polypoid colorectal neoplasms: classification, therapy and follow-up, World J. Gastroenterol. 21 (2015) 5149–5157.
[35] V.K. Dik, L.M.G. Moons, P.D. Slersema, Endoscopic innovations to increase the adenoma detection rate during colonoscopy, World J. Gastoenterol. 20 (2014) 2200–2211.
[36] K. Matsuoka, T. Kobayashi, F. Ueno, T. Matsui, F. Hirai, N. Inoue, J. Kato, K. Kobayashi, K. Kobayashi, K. Koganei, R. Kunisaki, S. Motoya, M. Nagahori, H. Nakase, F. Omata, M. Saruta, T. Watanabe, T. Tanaka, T. Kanai, Y. Noguchi, K. Takahashi, K. Watanabe, T. Hibi, Y. Suzuki, M. Watanabe, K. Sugano, T. Shimosegawa, Evidence-based clinical practice guidelines for inflammatory bowel disease, J. Gastroenterol. 53 (2018) 305–353.